Available online at www.eccomasproceedia.org
Eccomas Proceedia COMPDYN (2025) 1710-1722

ECCOMAS
Proceedia

COMPDYN 2025
10th ECCOMAS Thematic Conference on
Computational Methods in Structural Dynamics and Earthquake Engineering
M. Papadrakakis, M. Fragiadakis (eds.)
Rhodes Island, Greece, 15-18 June 2025

# REDUCED ORDER MODELING (ROM) EQUIPPED WITH RANDOM FOREST FOR STRUCTURAL DYNAMICS ANALYSIS

**Minyoung Yun[1], Mikhael Tannous[1], Chady Ghnatios[2], Trond Kvamsdal[3] and Francisco Chinesta[1]**

[1] Arts et Metiers Institute of Technology
Paris, France
e-mail: {minyoung.yun, mikhael.tannous, francisco.chinesta}@ensam.eu

[2] University of North Florida
Jacklsonville, Florida, USA
e-mail: chady.ghnatios@unf.edu

[3] Norwegian University of Science and Technology
Trondheim, Norway
e-mail: trond.kvamsdal@ntnu.no

**Abstract.** *This work introduces a novel minimally intrusive Proper Orthogonal Decomposition (POD)-based method for parametric dynamic structural analysis, addressing computational challenges posed by varying material properties such as Young's modulus or thickness. By leveraging two machine learning models—one predicting the mass matrix and the other the stiffness matrix for a given set of parameters—the approach significantly reduces computational demands while ensuring high accuracy. Validated through 65 case studies across different parameter sets, the methodology demonstrated stable and accurate displacement predictions, with most cases achieving errors within 1-2%. Larger discrepancies observed for the lowest thickness, caused by high oscillations in the dynamic modes' coefficient, were effectively mitigated using Savitzky-Golay filtering. These results underline the method's capability to provide parameter-specific reliability and computational efficiency, positioning it as a promising solution for real-time digital twin applications in dynamic structural analysis.*

**Keywords:** Reduced Order Modeling (ROM), Proper Orthogonal Decomposition, Machine Learning, Parametric Structural Dynamics, Digital Twin.

ISSN:2623-3347 
Peer-review under responsibility of the organizing committee of COMPDYN 2025.
doi: 10.7712/120125.12522.25674

## 1 INTRODUCTION

Dynamic structural analysis is critical for understanding how structures behave under time-varying loads, such as those caused by wind, earthquakes, or mechanical vibrations. In industries such as civil engineering, aerospace, and automotive design, accurately predicting structural responses is essential for ensuring safety, reliability, and performance [1, 2, 3]. However, traditional methods, such as the finite element method (FEM), often pose significant computational challenges, particularly when analyzing multiple parametric variations, such as changes in material properties or manufacturing parameters [4, 5, 6].

To address these challenges, model order reduction (MOR) techniques have emerged as a powerful approach, enabling structural analysis to be performed in reduced dimensions and thus accelerating computation time [7, 8, 9]. Among these, Proper Orthogonal Decomposition (POD) has demonstrated considerable success, particularly in static structural analysis, due to its efficiency in reducing the dimensionality of complex systems while preserving essential features of the solution [10, 11, 12, 13]. This success has motivated its exploration in dynamic structural problems, where the complexity increases due to time-dependent effects [14, 15]. Indeed, POD has been applied successfully to dynamic structural analysis in previous studies [16, 17, 18].

Despite these advances, dynamic structural analysis with parametric variations, such as changes in Young's modulus, thickness, or Poisson's ratio, remains underexplored. Such variations necessitate repeated analyses for different parameter sets, significantly increasing computational cost and limiting the practicality of traditional methods in real-time or large-scale applications. Moreover, while intrusive MOR techniques offer high fidelity and stability for large-scale problems, they require modifications to existing simulation codes, making them difficult to integrate with commercial finite element software. Non-intrusive MOR techniques, on the other hand, are easier to integrate but often require a large number of solution snapshots to achieve reliable performance, particularly in nonlinear contexts, and may still fall short of the accuracy provided by intrusive approaches.

This study proposes a minimally intrusive, POD-based methodology for parametric dynamic structural analysis that combines the strengths of both intrusive and non-intrusive MOR techniques. The methodology introduces machine learning models to predict the mass and stiffness matrices directly in the reduced space for a given set of parameters. This integration not only reduces computational costs but also ensures high accuracy and fidelity, addressing the limitations of existing methods in nonlinear and parametric contexts. By generating the inverted stiffness matrix in the reduced space with machine learning algorithms, the proposed approach enhances the applicability of reduced-order models while maintaining ease of integration and operation.

In the following sections, the proposed methodology is described in detail, followed by validation results based on 65 dynamic study cases with varying material properties. The results demonstrate the stability and accuracy of the displacement predictions, underscoring the potential of this approach for real-time dynamic digital twin applications. This work bridges the gap between computational efficiency and high-fidelity modeling, paving the way for advancements in parametric dynamic structural analysis.

# 2 METHODOLOGY

## 2.1 Governing Equation for Elastodynamics

The governing equation for the elastodynamics problem is expressed as:

$$\mathbf{M}\ddot{\mathbf{U}}(t) + \mathbf{D}\dot{\mathbf{U}}(t) + \mathbf{K}\mathbf{U}(t) = \mathbf{F}(t), \tag{1}$$

where:

- $\mathbf{M}$, $\mathbf{D}$ and $\mathbf{K} \in R^{N\times N}$ are respectively the mass, damping and stiffness matrices.
- $\mathbf{F}(t) \in R^{N\times 1}$: Time-dependent external force vector.
- $\mathbf{U}(t) \in R^{N\times 1}$: Time-varying nodal displacement vector.
- $\dot{\mathbf{U}}(t) \in R^{N\times 1}$: Time-varying nodal velocity vector.
- $\ddot{\mathbf{U}}(t) \in R^{N\times 1}$: Time-varying nodal acceleration vector.

Assuming small damping effects, the equation simplifies to:

$$\mathbf{M}\ddot{\mathbf{U}}(t) + \mathbf{K}\mathbf{U}(t) = \mathbf{F}(t). \tag{2}$$

Here, $\mathbf{M}$, $\mathbf{K}$, and $\mathbf{F}(t)$ retain their respective sizes, and the simplification focuses on the dominant mass and stiffness contributions. This formulation is central to analyzing the dynamic response of structures under time-dependent loading.

## 2.2 Proper Orthogonal Decomposition (POD)

Proper Orthogonal Decomposition (POD) is employed to represent high-dimensional data in a low-dimensional space, providing an efficient way to reduce computational complexity [19, 20]. This is achieved by identifying a set of orthogonal basis vectors that capture the dominant modes of the system.

The POD process begins with the Singular Value Decomposition (SVD) of the snapshots matrix:

$$\mathbf{U} = [\mathbf{U}^1, \mathbf{U}^2, \ldots, \mathbf{U}^Q] \in R^{N\times Q}, \tag{3}$$

where $N$ is the number of nodes, and $Q$ represents the total number of snapshots. The SVD decomposes $\mathbf{U}$ into three components:

$$\mathbf{U} = \mathbf{S}\mathbf{\Sigma}\mathbf{V}^T, \tag{4}$$

where:

- $\mathbf{S} = [\mathbf{s}^1, \mathbf{s}^2, \ldots, \mathbf{s}^Q] \in R^{N\times Q}$ is a matrix of orthogonal basis vectors.
- $\mathbf{\Sigma} = \text{diag}(\lambda^1, \lambda^2, \ldots, \lambda^Q) \in R^{Q\times Q}$ is a diagonal matrix of singular values ($\lambda^1 \geq \lambda^2 \geq \ldots \geq \lambda^Q \geq 0$).
- $\mathbf{V} = [\mathbf{v}^1, \mathbf{v}^2, \ldots, \mathbf{v}^Q] \in R^{Q\times Q}$ contains the right singular vectors.

The singular values $\lambda^i$ indicate the relative importance of the corresponding POD modes. Using the dominant $d$ modes ($d \ll N$), the original snapshots can be approximated as:

$$\mathbf{U} \approx \mathbf{B}\mathbf{\Phi}, \tag{5}$$

where $\mathbf{B} = [\beta^1, \beta^2, \ldots, \beta^d] \in R^{N\times d}$ and $\mathbf{\Phi} = [\phi^1, \phi^2, \ldots, \phi^Q] \in R^{d\times Q}$ is the expansion coefficient matrix representing the reduced coordinates.

Thus, POD achieves compression by truncating the original data to $d$ modes, retaining the most significant features while substantially reducing dimensionality.

### 2.3 Reduced formulation

When forces and displacements are correlated, both can be expressed in a reduced subspace $R^d$, where $d \ll N$ [24]. For a given combination of problem parameters $\mu^i$, the displacement $\mathbf{U}^i$ can be computed, forming a collection of solution snapshots that is used as explained in Section 2.2 to construct a reduced basis $\mathbf{V}$. From the latter, the displacement and acceleration vectors can be approximated as:

$$\mathbf{U} \approx \mathbf{V}\boldsymbol{\xi}, \tag{6}$$

$$\ddot{\mathbf{U}} \approx \mathbf{V}\ddot{\boldsymbol{\xi}}, \tag{7}$$

where $\boldsymbol{\xi} \in R^{d\times 1}$ is the reduced displacement vector.

Substituting the reduced displacement representation into the governing equation of elastodynamics gives:

$$\mathbf{M}\mathbf{V}\ddot{\boldsymbol{\xi}}(t) + \mathbf{K}\mathbf{V}\boldsymbol{\xi}(t) = \mathbf{F}(t). \tag{8}$$

To project this equation into the reduced subspace, the reduced basis $\mathbf{V}$ is used to obtain:

$$\mathbf{V}^T\mathbf{M}\mathbf{V}\ddot{\boldsymbol{\xi}}(t) + \mathbf{V}^T\mathbf{K}\mathbf{V}\boldsymbol{\xi}(t) = \mathbf{V}^T\mathbf{F}(t). \tag{9}$$

Defining the reduced mass matrix $\mathbf{M}_r = \mathbf{V}^T\mathbf{M}\mathbf{V}$, the reduced stiffness matrix $\mathbf{K}_r = \mathbf{V}^T\mathbf{K}\mathbf{V}$, and the reduced force vector $\mathbf{F}_r = \mathbf{V}^T\mathbf{F}(t)$, the reduced-order governing equation can be written as:

$$\mathbf{M}_r\ddot{\boldsymbol{\xi}}(t) + \mathbf{K}_r\boldsymbol{\xi}(t) = \mathbf{F}_r(t). \tag{10}$$

This reduced formulation significantly reduces the computational complexity while preserving the essential dynamics of the system.

### 2.4 Parametric reduced elastodynamics

#### 2.4.1 Construction of the reduced stiffness matrix

For parametric solutions, the reduced stiffness matrix corresponding to the $i$-th set of parameters $\mu^i$ is denoted as $\mathbf{K}_r^i$, where $i = 1, \ldots, P$. The reduced stiffness matrices are first expressed in vectorized form to facilitate the construction of a compact representation:

$$\mathbf{K}_r^i \rightarrow \boldsymbol{\chi}^i = \text{Vect}(\mathbf{K}_r^i), \tag{11}$$

where Vect$(\cdot)$ denotes the vectorization operator that transforms a matrix into a column vector.

The vectorized stiffness matrices $\boldsymbol{\chi}^i$ for all parameter combinations are concatenated into a matrix:

$$\boldsymbol{\chi} = [\boldsymbol{\chi}^1, \boldsymbol{\chi}^2, \ldots, \boldsymbol{\chi}^P] \in R^{d^2\times P}, \tag{12}$$

where $d$ is the dimension of the reduced basis, and $P$ is the number of parameter combinations.

Applying a truncated Singular Value Decomposition (SVD) to $\boldsymbol{\chi}$ yields the most relevant orthogonal singular vectors:

$$\boldsymbol{\chi} \approx \mathbf{A}\boldsymbol{\Psi}, \tag{13}$$

where:

- $\mathbf{A} = [\mathbf{A}^1, \mathbf{A}^2, \ldots, \mathbf{A}^m] \in R^{d^2 \times m}$: The basis matrix containing $m$ orthogonal singular vectors ($m \ll P$).
- $\boldsymbol{\Psi} \in R^{m \times P}$: The coefficients of the reduced representation for each parameter set.

Using this orthogonal basis, the vectorized stiffness matrices for new parameter sets can be approximated as:

$$\boldsymbol{\chi}^i \approx \mathbf{A}\boldsymbol{\psi}^i, \tag{14}$$

where $\boldsymbol{\psi}^i$ is the coefficient vector for the parameter set $\mu^i$.

To predict $\boldsymbol{\chi}^i$ for unseen parameter values, a Random Forest regression model is employed. The parameters $\mu^i$ serve as input features, and the model outputs $\boldsymbol{\psi}^i$, enabling the reconstruction of $\boldsymbol{\chi}^i$ using the orthogonal basis $\mathbf{A}$. Once $\boldsymbol{\chi}^i$ is predicted, it can be reshaped into matrix form to recover $\mathbf{K}_r^i$.

#### 2.4.2 Construction of the reduced mass matrix

The same methodology is applied to construct and predict the reduced mass matrices $\mathbf{M}_r^i$. The reduced mass matrices are first vectorized:

$$\mathbf{M}_r^i \rightarrow \boldsymbol{\eta}^i = \text{Vect}(\mathbf{M}_r^i), \tag{15}$$

and the corresponding vectorized forms are assembled into a matrix:

$$\boldsymbol{\eta} = [\boldsymbol{\eta}^1, \boldsymbol{\eta}^2, \ldots, \boldsymbol{\eta}^P] \in R^{d^2 \times P}. \tag{16}$$

Applying a truncated SVD to $\boldsymbol{\eta}$ provides the reduced basis for the mass matrices:

$$\boldsymbol{\eta} \approx \mathbf{C}\boldsymbol{\Theta}, \tag{17}$$

where $\mathbf{C}$ is the basis matrix for the mass matrices, and $\boldsymbol{\Theta}$ contains the reduced coefficients.

A Random Forest regression model predicts the coefficients $\boldsymbol{\theta}^i$ for new parameter sets $\mu^i$. Using these predictions, the vectorized mass matrix $\boldsymbol{\eta}^i$ is reconstructed as:

$$\boldsymbol{\eta}^i \approx \mathbf{C}\boldsymbol{\theta}^i, \tag{18}$$

which is then reshaped into matrix form to yield the reduced mass matrix $\mathbf{M}_r^i$.

#### 2.4.3 Summary

This approach ensures efficient and accurate construction of both the reduced stiffness and mass matrices for parametric variations. By leveraging Random Forest regression, the methodology seamlessly integrates machine learning predictions into the reduced-order modeling framework, enabling rapid evaluation of parametric solutions.

### 2.5 The Savitzky-Golay Filter

The Savitzky-Golay filter is a widely recognized smoothing technique commonly used in signal processing and sensing data applications [21, 22, 23]. This filter operates by fitting successive subsets of data with a polynomial of a specified degree, thereby preserving key features such as local maxima and minima while reducing noise.

In this study, the Savitzky-Golay filter was applied to the coefficients of the reduced basis for each parameterized case. The filter involves two critical parameters:

- **Window Length ($w$):** This parameter defines the number of data points considered in each subset of the data. A larger window length results in a smoother output but may risk oversmoothing important features, while a smaller window length retains finer details but may not sufficiently reduce noise.

- **Polynomial Order ($p$):** This parameter specifies the degree of the polynomial used to fit the data within each window. Higher-order polynomials provide greater flexibility in capturing variations but may introduce artifacts if the order is too high relative to the data's characteristics.

The application of the filter resulted in significant improvements in the smoothness of the coefficients, effectively mitigating high-frequency noise and oscillations. The smoother coefficients directly contributed to a reduction in errors observed in displacement predictions.

## 3 APPLICATION EXAMPLE

This example demonstrates the application of the proposed minimally intrusive approach to reduce the dimensionality of displacement snapshots, which represent the structural response of a plate subjected to dynamic loading. The setup consists of a square plate with its edges constrained to prevent movement, subjected to a time-dependent vertical concentrated point force, $\mathbf{F}(t)$, at its midpoint, as depicted in Figure 1. The applied force is defined as:

$$\mathbf{F}(t) = -500\sin(\pi t). \tag{19}$$

Numerical simulations are performed using a commercial finite element software to generate displacement data for each time increment. For each study case, displacement vectors are collected at every time step. The total number of snapshots is calculated as:

$$\text{Total snapshots} = \text{Number of study cases} \times \text{Snapshots per case}.$$

The displacement snapshots are processed using the POD methodology to extract dominant modes, which provide a compact representation of the dynamic structural behavior. Material properties, including Young's modulus ($E$), thickness ($\epsilon$), and Poisson's ratio ($\nu$), are varied within the following ranges: $E^i \in [100, 300]$ GPa, $\epsilon^i \in [1, 10]$ mm, and $\nu^i \in [0.3, 0.5]$.

Time integration is conducted using the Newmark-beta method with parameters $\beta = 0.25$ and $\gamma = 0.5$. To refine the POD coefficients obtained from time-integration, the Savitzky-Golay filter is applied with a window length of $w = 51$ and a polynomial order of $p = 3$. This filtering process effectively addresses the undulations observed in cases with lower plate thickness, such as Case1 (1 mm thickness), as shown in Figure 2. The blue line represents the dominant POD coefficient before smoothing, while the red line shows the filtered results, ensuring smoother coefficients.

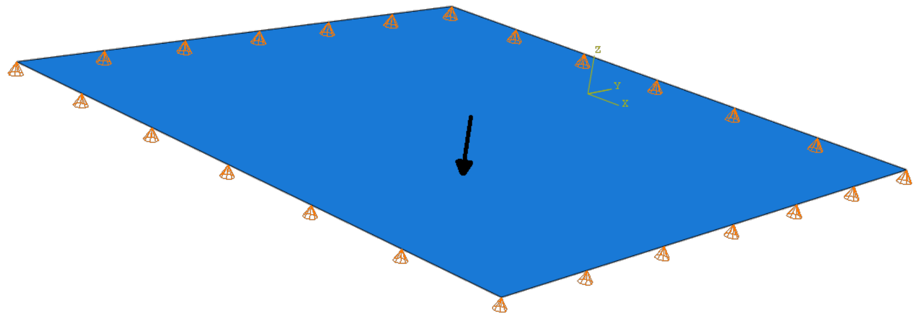

Figure 1: Schematic of a simply supported square plate under a time-dependent concentrated point load.

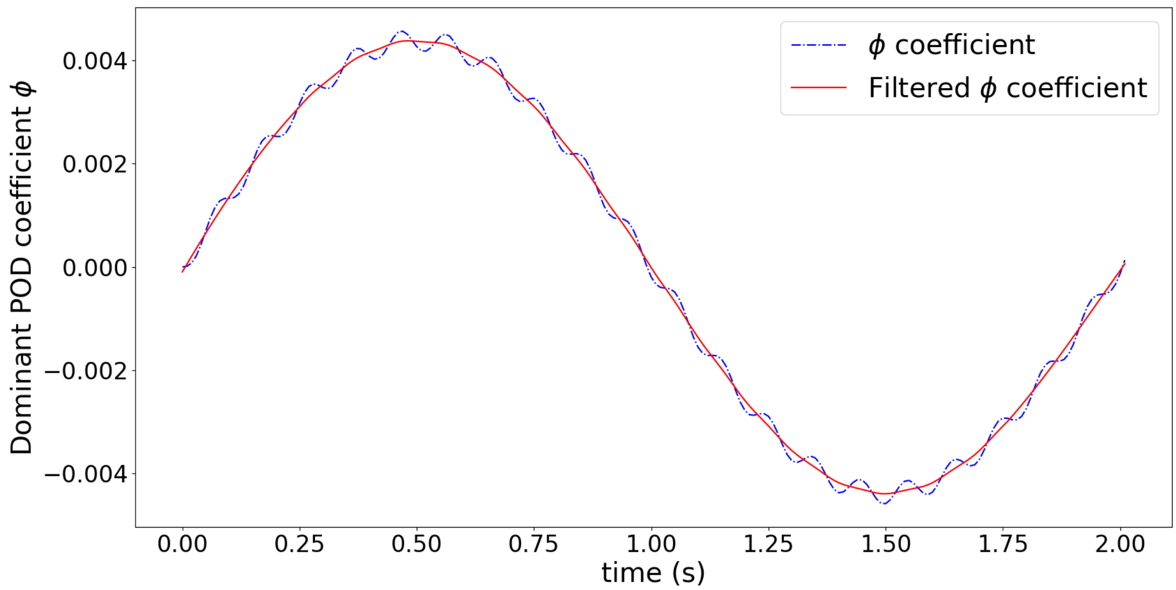


Figure 2: Time evolution of the dominant POD coefficient for Case1 (1 mm thickness) before and after smoothing using the Savitzky-Golay filter.

The smoothed coefficients are then multiplied by their respective POD modes to reconstruct the displacement fields. This reconstructed displacement is compared with the reference solution for validation. Figure 3 shows the comparison of the predicted and reference displacements in all directions ($x$, $y$, $z$) for a specific time step at which the displacement reaches its maximum value. A zoomed-in view of the indicated region in Figure 3 is provided in Figure 4, revealing excellent agreement between the predicted and reference displacements.

Displacement predictions in the $z$-direction, identified as the dominant direction of movement, are presented in Figure 5 for all time steps. Figure 6 further illustrates the displacement at the final time step. The latter two figures demonstrate the accuracy of the predicted results over both space and time.

The elastic energy, used as a metric for evaluating prediction accuracy, is compared between the reference and predicted solutions for all 10 time steps in Case1 (Figure 7). Relative errors in elastic energy across all 65 cases are summarized in Figure 8, where the error corresponds to the time step with the maximum deviation. The maximum error remains within 6%, with the largest deviations observed in cases with lower plate thickness due to sensitivity in time integration results.

This analysis demonstrates the effectiveness of the proposed minimally intrusive, projection-

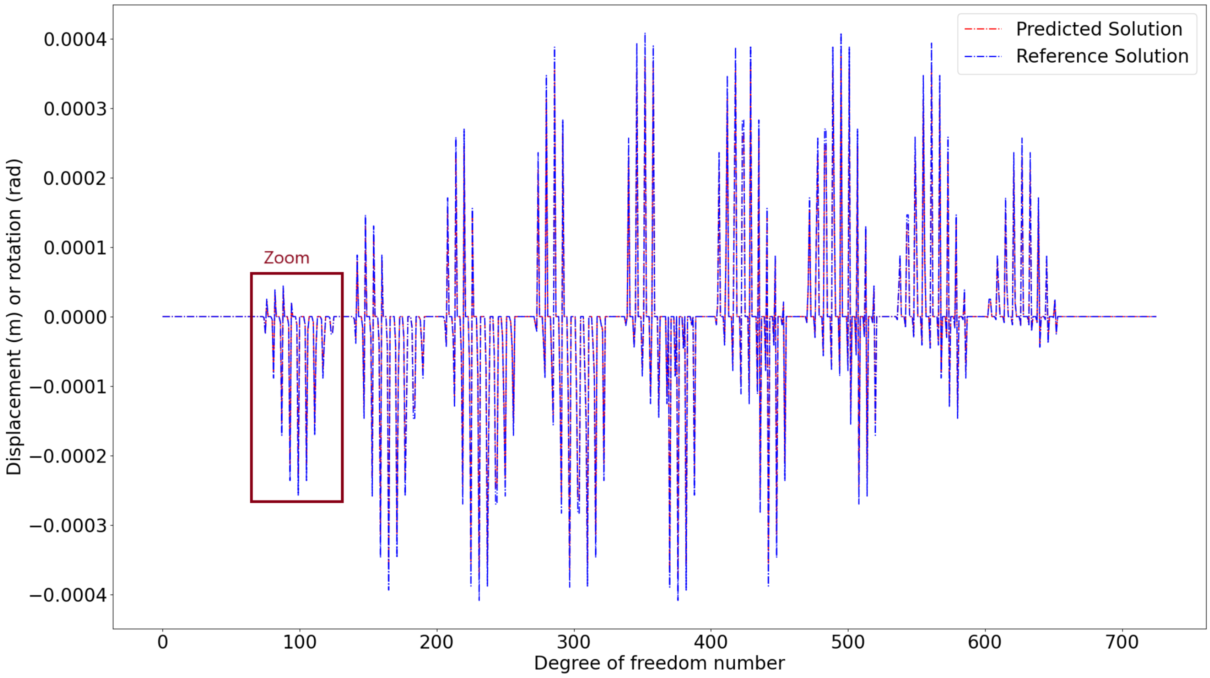


Figure 3: Comparison of displacement predictions with reference solutions in all directions ($x$, $y$, $z$) at the time step corresponding to the maximum displacement for Case1.

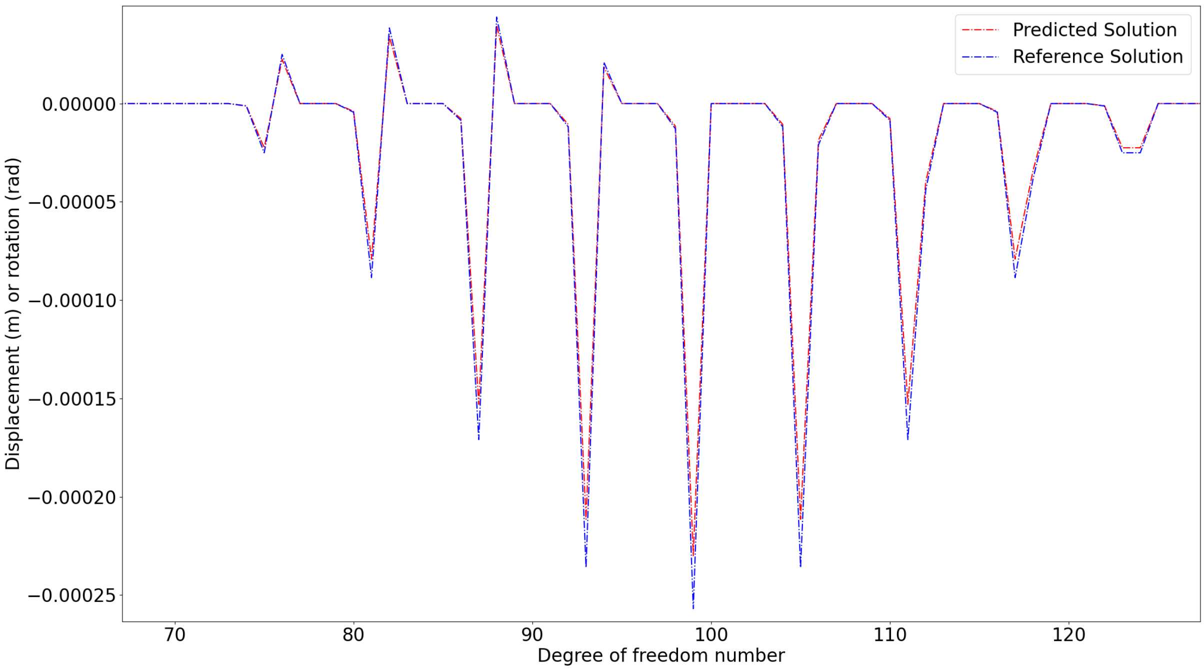


Figure 4: Zoomed view of the indicated region in Figure 3 for Case1, highlighting the accuracy of the displacement predictions.

based, reduced order modeling methodology in accurately predicting dynamic structural responses while maintaining computational efficiency, particularly in scenarios involving parametric variations in material properties.

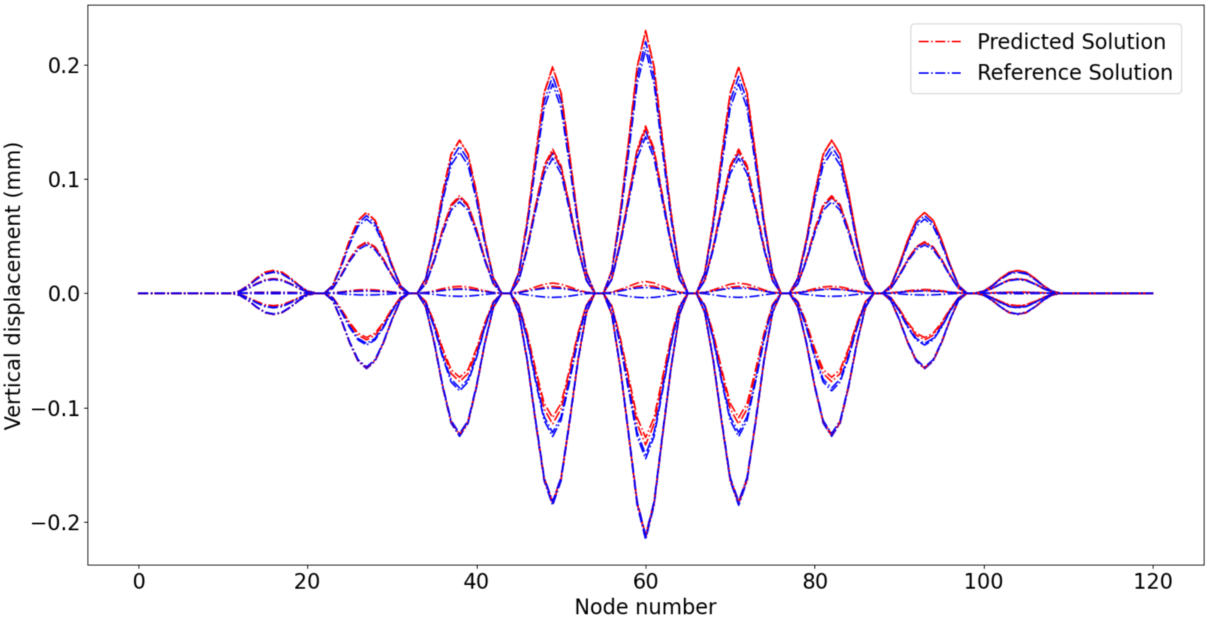


Figure 5: Comparison of $z$-direction displacement predictions with reference solutions for all time steps in Case1.

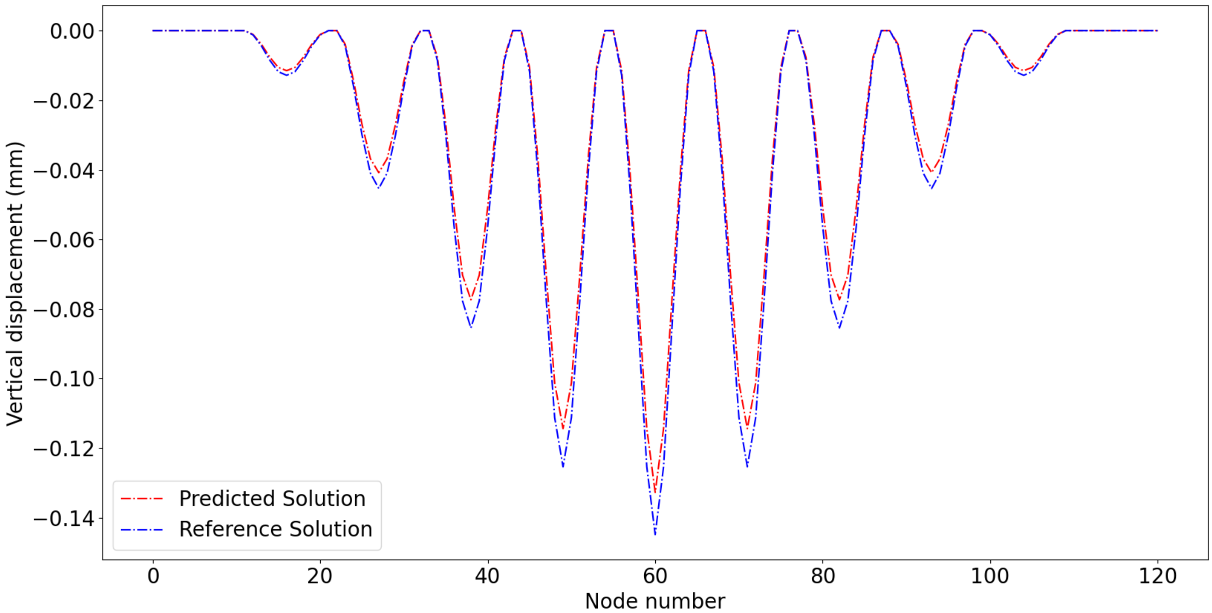


Figure 6: Predicted and reference $z$-direction displacements for Case1 at the final time step.

## 4 CONCLUSION

This work presents a novel minimally intrusive Proper Orthogonal Decomposition (POD) method for parametric dynamic structural analysis. The method was validated using 65 cases, in which material properties—such as Young's modulus, thickness, and Poisson's ratio—were varied within predefined ranges to assess the robustness of the approach. A key aspect of this methodology was the incorporation of two machine learning models: one for predicting the mass matrix and another for predicting the stiffness matrix. This allowed for efficient and accurate modeling of the system dynamics without the need for full recalculation of these matrices, which contributes to the efficiency of the minimally intrusive approach.

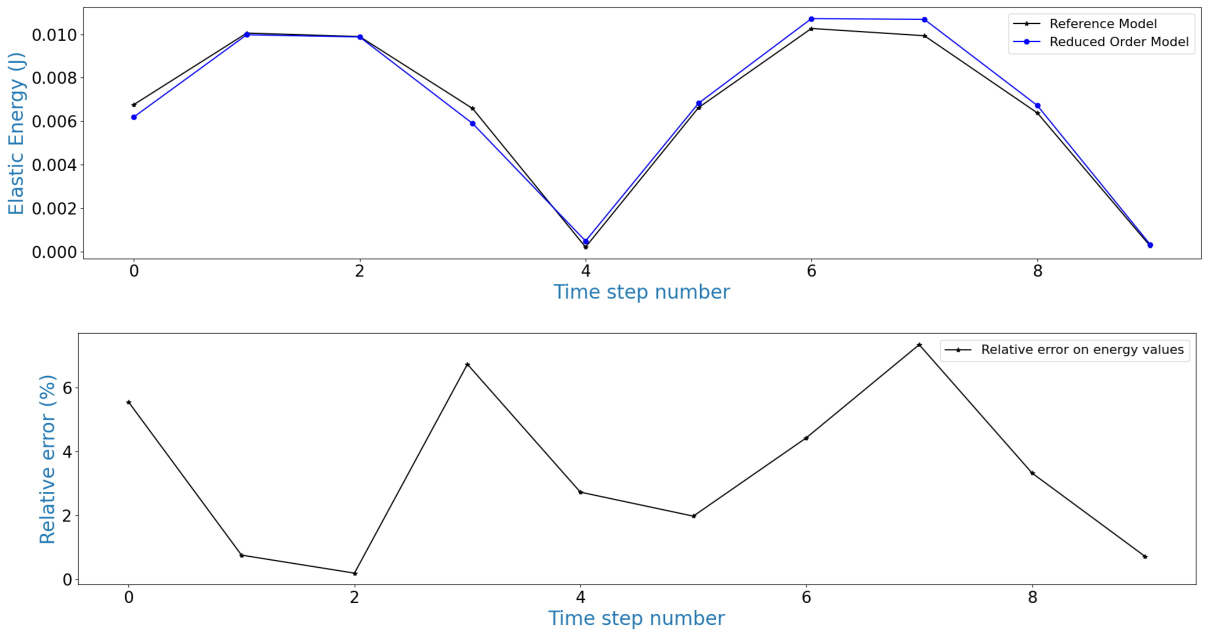


Figure 7: Comparison of elastic energy predictions with reference solutions over 10 time steps for Case1.

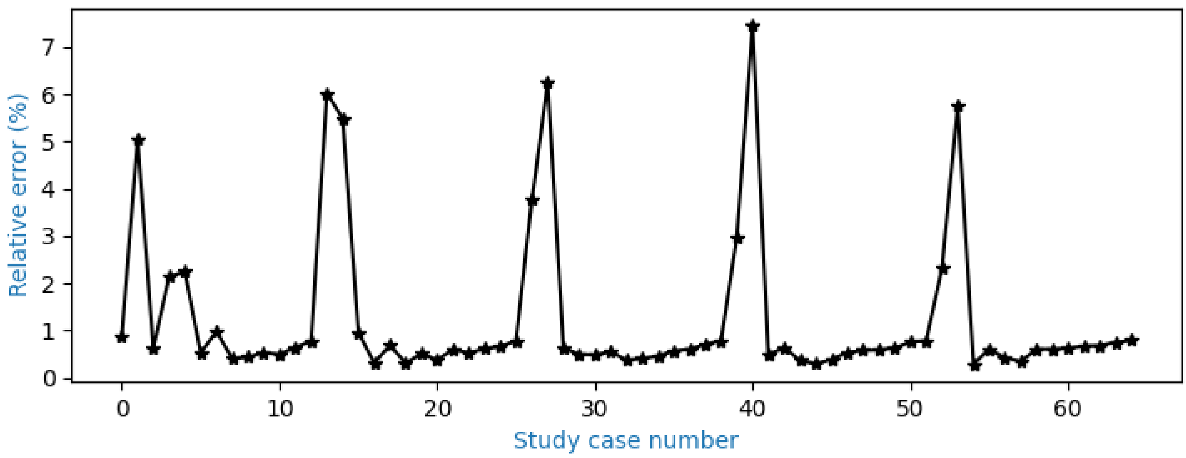


Figure 8: Relative errors in elastic energy for all 65 cases, showing the maximum error for each case.

The methodology successfully achieved stable displacement predictions, which was the primary objective of this study. In the majority of the 65 cases, the relative error was limited to 1-2%, with exceptions mainly in cases with the lowest thickness, where higher discrepancies were observed. These larger errors were attributed to the high undulations present in the coefficients during the initial time integration process. However, this issue was significantly mitigated through the application of Savitzky-Golay filtering, resulting in improved accuracy of the predictions. Overall, the proposed minimally intrusive POD method has demonstrated its capability to reliably handle parametric variations, maintaining accuracy while reducing computational costs.

The application of this methodology, inspired by its success in static structural analysis, demonstrates its feasibility for use in dynamic cases, which is crucial for digital twin technology. By efficiently modeling dynamic responses with varying material properties and incorporating machine learning for predicting mass and stiffness matrices, this approach significantly reduces computational costs. This makes real-time analysis and updates possible, a key requirement for digital twins. The demonstrated stability and accuracy in displacement predictions highlight the potential for integrating this method into digital twin systems for dynamic structural analysis in various fields, such as civil infrastructure and aerospace.

## ACKNOWLEDGMENTS

This project has received funding from:

- the European Defense Fund (EDF) under grant agreement 101103257 dTHOR-EDF-2021-NAVALR-2 (https://dthor.eu/)
- the European Union's Horizon Europe Research and Innovation program under Grant Agreement No. 101091449 PIONEER.

## REFERENCES

[1] Singarajan Nagammal Vijayan and Sathiavelu Sendhilkumar. Structural analysis of automotive chassis considering cross-section and material. *International Journal of Mechanical Engineering and Automation*, 2(8):370–376, 2015.

[2] Banoth Ganesh, B Vjay Kumar, and D Muppala. Design and structural analysis of aircraft floor panel. *International Journal of Advanced Engineering and Global Technology*, 3(12):1451–1460, 2015.

[3] Roberto d'Ippolito, Stijn Donders, Luc Hermans, HV der Auweraer, and Dirk Vandepitte. Reliability-based design optimization for aerospace and automotive structures. *The Marie Curie Fellowships Annals*, 4, 2006.

[4] H Benaroya and M Rehak. Finite element methods in probabilistic structural analysis: a selective review. 1988.

[5] Serban Georgescu, Peter Chow, and Hiroshi Okuda. Gpu acceleration for fem-based structural analysis. *Archives of Computational Methods in Engineering*, 20:111–121, 2013.

[6] Aadya Mishra, Sourav Pal, G Malhi, and PRABHAT Singh. Structural analysis of uav airframe by using fem techniques: A review. *International Journal of Mechanical and Production, ISSN*, 10:2249–6890, 2020.

[7] Zhen Li, Yao Lin Jiang, and Hong liang Mu. Parametric model order reduction based on parallel tensor compression. *International Journal of Systems Science*, 52:2201–2216, 2021.

[8] Luca Rosafalco, Matteo Torzoni, Andrea Manzoni, Stefano Mariani, and Alberto Corigliano. Online structural health monitoring by model order reduction and deep learning algorithms. *Computers and Structures*, 255, 10 2021.

[9] Van Bo Nguyen, Si Bui Quang Tran, Saif A. Khan, Jiawei Rong, and Jing Lou. Pod-deim model order reduction technique for model predictive control in continuous chemical processing. *Computers and Chemical Engineering*, 133, 2 2020.

[10] R. Semaan. Optimal sensor placement using machine learning. *Computers and Fluids*, 159:167–176, 12 2017.

[11] Clarence W Rowley, Tim Colonius, and Richard M Murray. Model reduction for compressible flows using pod and galerkin projection. *Physica D: Nonlinear Phenomena*, 189(1-2):115–129, 2004.

[12] Rut Vitkovicova, Yoshifumi Yokoi, and Tomas Hyhlik. Identification of structures and mechanisms in a flow field by pod analysis for input data obtained from visualization and piv. *Experiments in Fluids*, 61:1–21, 2020.

[13] Jan Awrejcewicz, Vadim A Krys' ko, Alexander F Vakakis, Jan Awrejcewicz, Vadim A Krys' ko, and Alexander F Vakakis. Order reduction by proper orthogonal decomposition (pod) analysis. *Nonlinear Dynamics of Continuous Elastic Systems*, pages 177–238, 2004.

[14] Gorka Garate, Isabel Harismendy, Oihane Echeverria-Altuna, and Julián Estévez. A dynamic data driven application system for real-time simulation of resin transfer moulding processes. *International Journal of Material Forming*, 15, 5 2022.

[15] Syuzanna Sargsyan, Steven L. Brunton, and J. Nathan Kutz. Nonlinear model reduction for dynamical systems using sparse sensor locations from learned libraries. *Physical Review E - Statistical, Nonlinear, and Soft Matter Physics*, 92, 9 2015.

[16] Saeed Eftekhar Azam and Stefano Mariani. Investigation of computational and accuracy issues in pod-based reduced order modeling of dynamic structural systems. *Engineering structures*, 54:150–167, 2013.

[17] Jun Liang, Bence Kato, and Ying Wang. Constructing simplified models for dynamic analysis of monopile-supported offshore wind turbines. *Ocean Engineering*, 271:113785, 2023.

[18] Karim Mostafa, Ioannis Zisis, and Mohamed A Moustafa. Machine learning techniques in structural wind engineering: A state-of-the-art review. *Applied Sciences*, 12(10):5232, 2022.

[19] Y. C. Liang, H. P. Lee, S. P. Lim, W. Z. Lin, K. H. Lee, and C. G. Wu. Proper orthogonal decomposition and its applications - part i: Theory. *Journal of Sound and Vibration*, 252:527–544, 5 2002.

[20] Julien Weiss. A tutorial on the proper orthogonal decomposition. In *AIAA aviation 2019 forum*, page 3333, 2019.

[21] Jin Chen, Per Jönsson, Masayuki Tamura, Zhihui Gu, Bunkei Matsushita, and Lars Eklundh. A simple method for reconstructing a high-quality ndvi time-series data set based on the savitzky–golay filter. *Remote sensing of Environment*, 91(3-4):332–344, 2004.

[22] Deepshikha Acharya, Asha Rani, Shivangi Agarwal, and Vijander Singh. Application of adaptive savitzky–golay filter for eeg signal processing. *Perspectives in science*, 8:677–679, 2016.

[23] Sunder Ram Krishnan and Chandra Sekhar Seelamantula. On the selection of optimum savitzky-golay filters. *IEEE transactions on signal processing*, 61(2):380–391, 2012.

[24] Kunihiko Taira, Steven L. Brunton, Scott T. M. Dawson, Clarence W. Rowley, Tim Colonius, Beverley J. McKeon, Oliver T. Schmidt, Stanislav Gordeyev, Vassilis Theofilis, and Lawrence S. Ukeiley. Modal analysis of fluid flows: An overview. *AIAA Journal*, 55(12):4013–4041, 2017.